CONSOLIDATION OF THERMOPLASTIC COMPOSITE PREFORMS VIA TAILORED OVERBRAIDING

Jessica Lavorata[1] and Jan-Anders E. Mansson[2]

[1,2] Manufacturing and Design Laboratory, https://www.purdue.edu/engineering/mdlab/
Purdue University, 1105 Endeavour Drive, West Lafayette IN 47906

[1] jlavorata@purdue.edu
[2] jmansson@purdue.edu

Keywords: tow, overbraiding, consolidation, hybrid molding

ABSTRACT

This paper introduces a new manufacturing method using continuous fiber thermoplastic preforms consolidated then formed into a three-dimensional skeleton for tailored structural reinforced injection-molded parts. The preform is produced as a linear composite preform rod, called M-TOW®, which allows for unique functionality, as well as reduced manufacturing costs and cycle times of the molded parts. The goal of the work is to investigate the consolidation behavior of the M-TOW® preform to better predict its mechanical performance in structural applications. Using Darcy's law for non-Newtonian fluids in transverse fiber beds, this study extends on existing models to characterize the "squeeze-out" of resin in the M-TOW® during consolidation. Successful modeling of the influence of the circumferential pressure applied by the overbraid on the radius and volume fraction of the fiber bundle was achieved. For a representative tow sample, consolidation improved by ~20% when a circumferential "squeeze" pressure was applied using an overbraid tension of 0.3 MPa·m. The model can be extended to predict consolidation and performance for tows of various constituents, radii and fiber volume fraction.

This relationship reduces the need for in-depth microscopy and can be used to motivate a robust processing window for this novel manufacturing line. By having a better understanding of how the volume fraction changes within the tow, more accurate predictions of mechanical properties can be made to improve the reliability of the CAE. Furthermore, it expands the application areas where M-TOW® and hybrid molding can be confidently and cost-effectively be implemented. The findings on consolidation behavior can be applied to improve the processing window and to predict mechanical performance for M-TOW® and hybrid molding applications. The outcomes suggest that the implementation of M-TOW® is a promising new manufacturing approach for locally reinforced structural injection-molded parts using continuous fiber thermoplastic preforms.

1 INTRODUCTION

Hybrid molded composites are becoming a popular approach to reduce part weight while also maintaining a short cycle time and an elevated mechanical performance. While several different approaches have been taken to hybrid molding [1–9], this work utilizes continuous fiber thermoplastic preforms formed into a three-dimensional skeleton to locally reinforce structural injection-molded parts. This paper introduces a new manufacturing method that combats the elevated manufacturing costs and extensive cycle times normally associated with continuous fiber polymer composites. The approach used is by producing a linear thermoplastic composite preform rod, referred to as M-TOW® (Multi-tow) which can be formed into complex shapes to act as tailored structural reinforcement in injection-molded parts. Several studies have been performed confirming the improved mechanical properties that continuous fiber tow offers in molded parts [9–11], but none have looked at the consolidation evolution of the tow. This work investigates the consolidation of the M-TOW® preforms to support more accurate predictions of mechanical performance while designing with the tow preforms for structural applications.

Analyzing and modeling consolidation behavior in polymer composites has been studied extensively which allows for this work to extend on existing models to characterize the "squeeze-out" of resin from the continuous fiber prepreg during overbraided of the M-TOW®. Several works describe Newtonian flow through particles that are simply spherical [12–14] as well as slightly distorted shapes such as ellipses or kidney beans [15], [16]. The most similar applications to the M-TOW® line are pultrusion or filament winding where the fiber bundle cross section is circular and can be considered transversely isotropic. In these processes, the resin flows perpendicular through the aligned fiber bed and experiences a shear-thinning behavior at a high-rate of manufacturing [17]. Work by Cai et al. and Seo and Lee's model for radial resin flow into a cylindrical fiber bundle was the main inspiration for the model presented in this work [13], [18]. As seen in Figure 1, M-TOW® is unique because the resin is already present in the fiber bed in the initial prepreg form and the applied circumferential overbraiding pressure squeezes the resin outwards, which is contrary to a more conventional inwards infiltration of dry fiber beds.

(a) flat tapes (b) transition to circular tow (c) circular M-TOW®

Figure 1: Illustration of M-TOW® material system which begins with (a) several prepreg tapes that are (b) compacted into a tow via an s-configuration roller unit then (c) consolidated via overbraiding to a tow with a cylindrical cross-section. The overbraiding squeezes out the resin, consolidating the continuous fibers of the prepreg.

The objective of this work was to gain a better understanding of the manner in which the overbraid affects the consolidation of the M-TOW®. The primary focus was determining the amount of resin squeezed out of the continuous fiber core when circumferential pressure from the overbraid was applied. Darcy's law and the Carman-Kozeny relationship were used to predict the flow behavior of the thermoplastic resin through the fibers within the M-TOW®.

2 METHODS

The production of hybrid molding with M-TOW® is divided into three process steps, from input material to finished part, as shown in Figure 2. First, the base constituents are determined. This fiber-polymer system is typically in the form of prepreg with unidirectional continuous fiber and a thermoplastic resin, however, functional components for conductivity, fluid transfer, sensing, etc. can also be integrated into the tow [19], [20]. This material is produced into M-TOW® on the M-TOW® manufacturing line, patented by EELCEE Ltd. [21]. In the M-TOW® cell, the tow is formed into three-dimensional preforms. These preforms are transferred to subsequent molding operations (e.g. compression, injection, etc.) for the polymer overmolding of the preform to produce the final structural part. The focus of this paper is on the consolidation of the base constituents during manufacturing on the M-TOW® line, therefore, the performance of the M-TOW® preforms after forming and molding are not discussed.

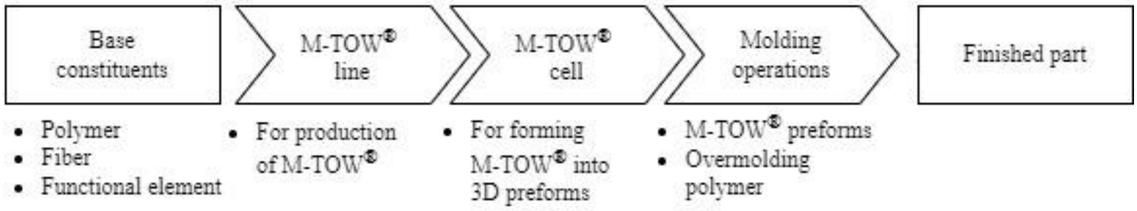

Figure 2: Diagram outlining full manufacturing concept for M-TOW® [19].

2.1 Process Overview

The M-TOW® manufacturing line consists of eight integrated units as shown in Figure 3 where each unit represents a unique stage of the M-TOW® production. The initial creel (stage a) holds the arrangement of the selected input tapes. Next in the oven (stage b), individual thermoplastic pre-impregnated tapes are heated above their melting temperature and compacted into a single unidirectional core. This stage provides the M-TOW® its overall compressed cross section. In stage c, dry fiber is overbraided onto the core tow to ensure its cylindrical geometry withstands the subsequent bending process with maintained consolidation and compaction. Using an extruder in stage d, a polymer coating could be applied to the surface of the tow which enhances bonding during subsequent additive molding operations. This stage is optional and was not included in the samples investigated in this study. In the subsequent line units, the resulting linear composite rod is cooled (stage e), advanced through the puller (stage f), cut to length (stage g) and stored (stage h) for forming in the M-TOW® cell. This paper focuses on stage c of the M-TOW® line where sufficient consolidation is achieved through the indirect pressures provided by the overbraiding process. The process is assessed by measurements of tow radius and fiber volume fraction as well as the distribution of the constituents within the tow.

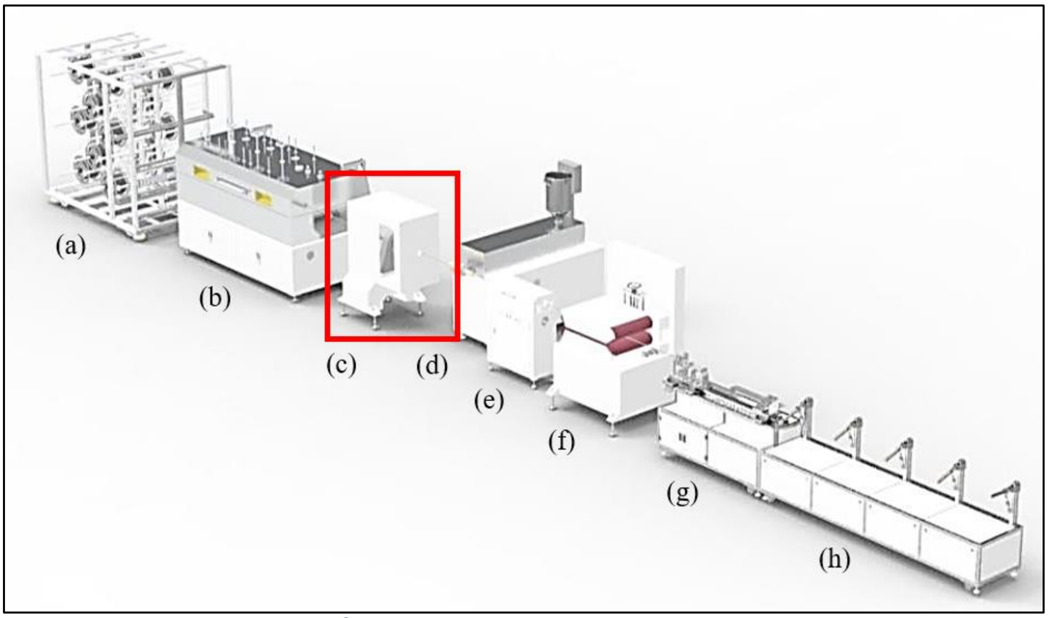

Figure 3: Overview of M-TOW® line. Components shown include a) creel, b) infrared oven, c) braider, d) extruder, e) cooler, f) puller, g) cutter, h) stacker. Image courtesy of EELCEE Ltd [21].

This manufacturing method will enable a cost-effective continuous fiber thermoplastic manufacturing comparison to other composite fabrication methods. When combined with current molding processes, M-TOW® reinforcement offers advances in structural efficiency and weight reduction while simultaneously providing the possibility of introducing and embedding other functional components for purposes such as conductivity, fluid transfer and sensing within complex shaped products.

2.2 Materials

The prepreg used for the M-TOW® core in this study was E-glass-reinforced polypropylene prepreg produced by LOTTE Chemical Corp with a fiber volume fraction (V_f) of 0.20. Four tapes with a cross-sectional area of 6.6 mm^2 were consolidated into tow with a final diameter of approximately 5 mm. The biaxial overbraid consisted of eight bobbins of dry 300 Tex E-glass fiber. An example of M-TOW® samples used is provided in Figure 4b.

2.3 Optical Microscopy

The samples were cut transverse to the fibers to observe the cross-section of the tow. After grinding and polishing, optical microscopy was performed on a Leica DMI 5000 M inverted microscope where images were taken at 10x resolution and stitched together to create a mosaic of the complete sample.

2.4 Consolidation Model

The amount of resin that was squeezed out from the core was modeled using basic assumptions about the process. The process was split into two basic stages, see Figure 4a, where stage one represents the tow before the circumferential "squeeze" pressure is applied and stage two represents the tow after pressure is applied. Stage one takes place when the unidirectional continuous fiber thermoplastic prepreg tow enters the braider. The tow is assumed to have the fibers and resin dispersed in a homogeneous manner into a circular cross-section. Additionally, the resin is above its T_m to allow for sufficient flow. Stage two is after pressure is applied by the overbraid. There are four assumptions that are made in stage two. Assumption one is that pressure is applied at the boundary of the fiber region. The second assumption is that the pressure exerted by the braid is uniformly distributed around the tow. Assumption three is that the core cools below T_m quickly, locking the consolidated fibers in place. The final assumption is that the fibers compact into a smaller-radius circle with higher volume fraction while the resin is displaced to form a resin-rich 'shell' around the fiber bundle.

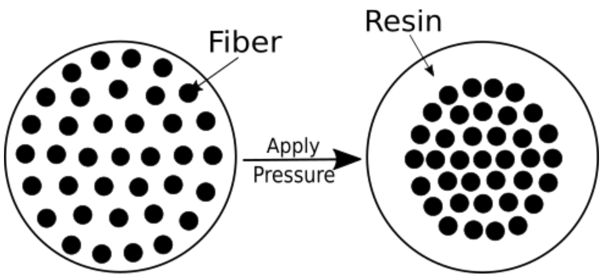

(a)

(b)

Figure 4: (a) Schematic of the fiber bundle consolidating as pressure is applied. Stage one is on the left before pressure is applied while stage two is represented on the right after pressure is applied. (b) Side view of a representative sample of M-TOW® with polymer squeeze-out promoted by the overbraid.

Following work done by Cai et al. [13], the pressure exerted by the braid on the fiber bundle is determined by Equation (1)

$$P_b = \frac{Fcos^2\alpha}{r_f} \quad (1)$$

where F is the winding tension force of one braid layer, α is winding angle, which was measured after processing, r_f is fiber bundle radius, and P_b is the circumferential pressure exerted by braid. A schematic displaying the coordinate system used for the model is shown in Figure 5. Equation (1) assumes that the force applied by the tensioned overbraid is in equilibrium with the radial pressure exerted on the tow. This P_b is a finite consolidation pressure at the boundary of the fibers while the outer tow boundary is atmospheric pressure. This pressure gradient throughout the tow radius causes the molten resin to flow towards the surface of the tow while the fiber bundle consolidates in the center.

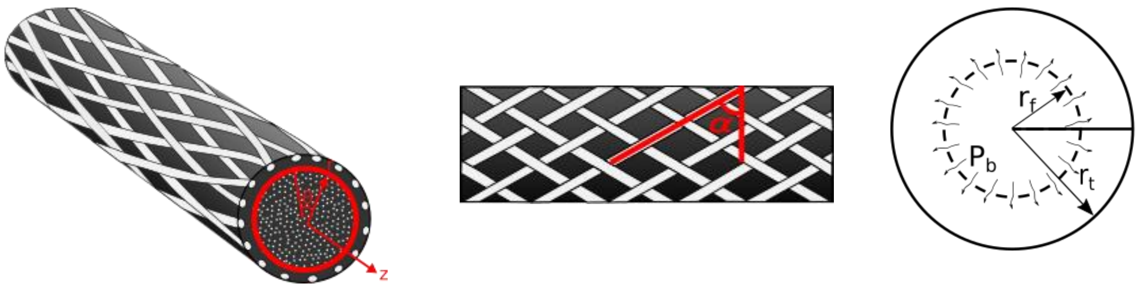

(a) (b) (c)

Figure 5: Schematic of the overbraiding process of cylindrical M-TOW® (a) coordinate system and (b) helical wind angle α, adapted from [13]. The radial resin flow is modeled (c) where P_a = atmospheric pressure, P_b = braid pressure, r_t = tow radius r_f = fiber bundle radius.

First, we assume that the circumferential braid pressure is applied uniformly inside the central fiber region r_f. The pressure distribution is expressed in Equation (2) using radial coordinates

$$P(r) = P_b\theta(r - r_f) \quad (2)$$

where $\theta(r - r_f)$ is a step function where: inside r_f, $\theta = 1$ and outside r_f, $\theta = 0$. Next, Darcy's law is used to describe the flow of the polymer melt as it is squeezed from the fiber bundle. The characteristics of the M-TOW® manufacturing process proposed the use of the shear thinning law [17]. The equivalent form of Darcy's law for non-Newtonian fluids (power law shear thinning) is expressed in Equation (3)

$$q = -K\left(\frac{\nabla P}{\mu}\right)^{\frac{1}{n}} \quad (3)$$

where μ is the zero-shear rate viscosity and n is the shear thinning power-law constant. The values used for the polypropylene are $\mu = 500\ Pas$ and $n = 0.6$ [17]. K is the permeability of the fiber bed which depends on fiber volume fraction, V_f. As shown in Figure 5c, the final fiber radius depends on V_f as the inner fiber radius cannot compact. Gutowski et al. proposes the Carman-Kozeny equation for flow transverse to fibers to relate permeability K to V_f in Equation (4) [22].

$$K = \frac{r_s^2\left[\sqrt{\frac{V_a'}{V_f}} - 1\right]^3}{4k'\left[\frac{V_a'}{V_f} + 1\right]} \quad (4)$$

where r_s is the individual fiber radius, V_a' is the impermeable volume fraction (~0.9 for close packed circles), and k' is the Carman-Kozeny constant. Following previous work by Gibson and Mansson [12], k' is assigned a value of 10 as the volume fraction range of 0.2 – 0.6 is of interest in this study. The volume fraction can be deduced by conservation of fibers as the fiber region shrinks. For a tow with an initial fiber volume fraction of $\mathrm{V_{f,0}}$, the instantaneous volume fraction is in Equation (5)

$$\mathrm{V_f}(r_f) = \mathrm{V_{f,0}} \frac{{r_{f,0}}^2}{r_f^2} \tag{5}$$

Using Darcy's law with the stepwise pressure distribution yields a volume flux which is localized to the surface as shown in Equation (6)

$$q(r) = K\left(\frac{P_b}{\mu}\right)^{\frac{1}{n}} \delta(r - r_f) \tag{6}$$

Interpreting the flux of resin as the negative rate of change of the fiber region area, we obtain the following time derivative of the fiber region radius in Equation (7)

$$\frac{dr_f}{dt} = -K\left(\mathrm{V_f}(r_f)\right)\left(\frac{F\cos^2\alpha}{\mu r_f}\right)^{\frac{1}{n}} \tag{7}$$

This differential equation allows us to predict the consolidation of the fibers in the M-TOW® over time. Additionally, initial conditions such as initial tow radius $r_{f,0}$ and initial fiber volume fraction $V_{f,0}$ can be modified to extend the model to tows with different properties and configurations.

3 RESULTS AND DISCUSSION

Figure 5c shows a schematic of the expected behavior of the tow upon the application of the circumferential overbraiding pressure at the boundary of the fiber region; the force from the braid causes the resin to "squeeze-out" from the fibers, thus increasing the fiber volume fraction of the fiber bundle while maintaining the tows' radius and overall shape. The micrograph shown in Figure 6 confirms that this is essentially what is taking place experimentally and that the circular model derived above is a relevant approach to predict the consolidation of the M-TOW®. The variation in the tow's final shape is due to gravity acting on the molten resin. However, this variation is only seen in the resin regions of the tow while the fiber bundle remains cylindrical, confirming that pressure is evenly distributed by the overbraid.

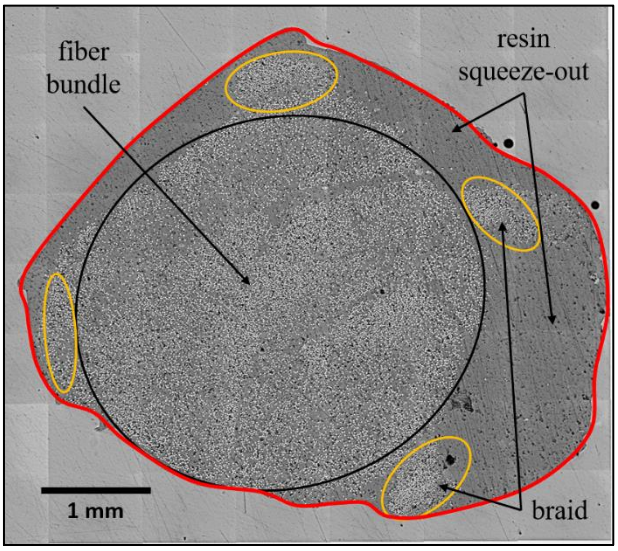

Figure 6: Micrograph of M-TOW® cross section. The fiber bundle is traced in black, the overbraid is encircled in yellow, and the entire tow perimeter is enclosed in red.

Applying Equation (7) to the initial parameters specific to the M-TOW® line, the evolution of the fiber bundle radius is shown in Figure 7, where a braid tension F of 0.3 MPa·m and an initial fiber bundle radius r_{f0} of 2.5 mm was used. The initial volume fraction of the representative experimental tow was low (~0.18) which allowed for a greater decrease in radius to be observed (Figure 7a) and increase in fiber volume fraction (Figure 7b). Experimental data is included in Figure 7 where the measured values populate around a final radius of the fiber region of approximately 2.1 mm. The exact time that this consolidation takes place is estimated, but comparison to the model suggests that the squeeze-out process occurs over roughly one second. Figure 7 also extends the model to predict the consolidation behavior in tows with higher V_f in the same amount of time. If a greater change in r_f and V_f is desired at higher initial volume fractions, greater pressure must be exerted or more time must be allowed for the resin to flow before solidifying. This is because the permeability decreases for higher volume fractions.

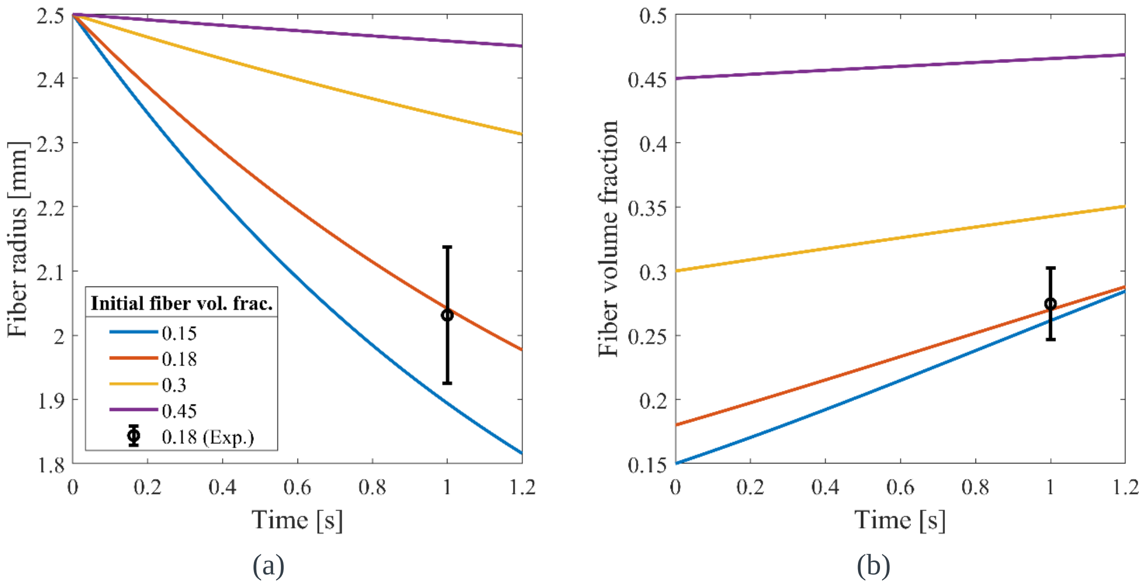

Figure 7: Applying equation (7), (a) the internal fiber bundle radius r_f decreases at a rate proportional to the initial fiber volume fraction and (b) V_f increases as pressure is applied. Experimental data was taken at ~0.18 V_f with error bars representing one standard deviation.

Figure 8 extends the model to show the characteristic evolution curves for tows of various initial radius. The representative experimental sample shows approximately a 18% reduction in the radius of the fiber region (Figure 8a) which transfers to a 20% increase in V_f (Figure 8b). Because of the $1/r_f$ dependence of the braid pressure on fiber region radius, however, we find that larger tows consolidate less in a given amount of time.

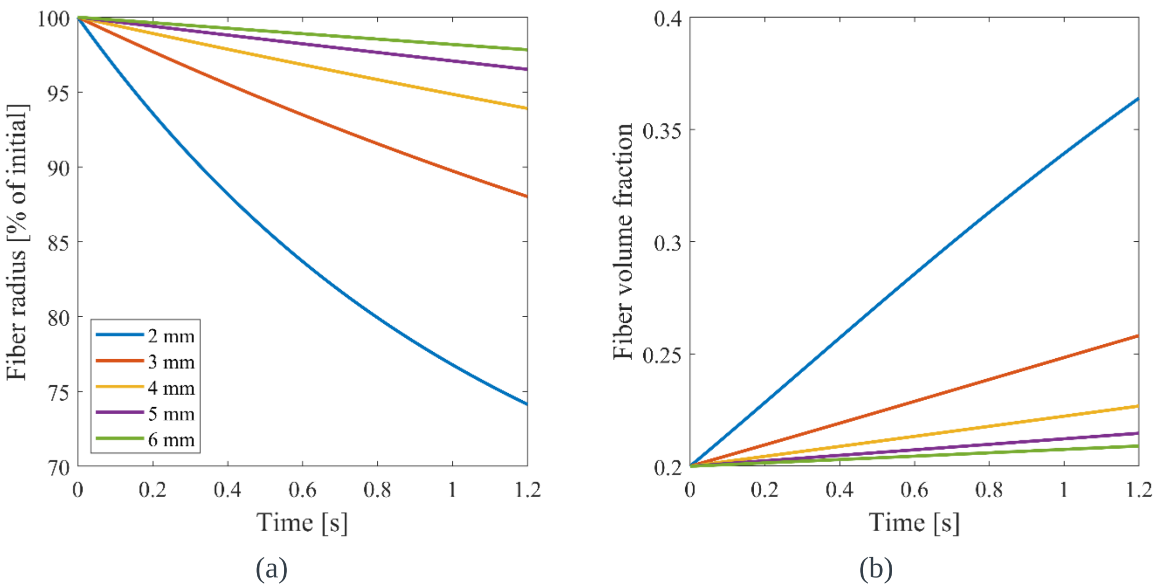

Figure 8: Time evolution of fiber region radius and the resulting V_f in the fiber region. These are both shown for various initial tow radii with an initial fiber volume fraction of 0.20.

These trends can be seen more clearly in Figure 9, which shows the dependence of the area reduction on initial tow radius (Figure 9a) and initial fiber volume fraction (Figure 9b). This measure of area reduction is equivalent to the fraction of the cross-section which is squeezed out of the fiber region, i.e. the resin rich area. Figure 9b shows the same measure plotted against the initial fiber volume fraction. Increasing the tow radius or volume fraction both lead to decreased consolidation. Higher V_f are less permeable and thus consolidate less in a given amount of time. Additionally, the constant circumferential braid pressure applied has a smaller influence on larger initial radii.

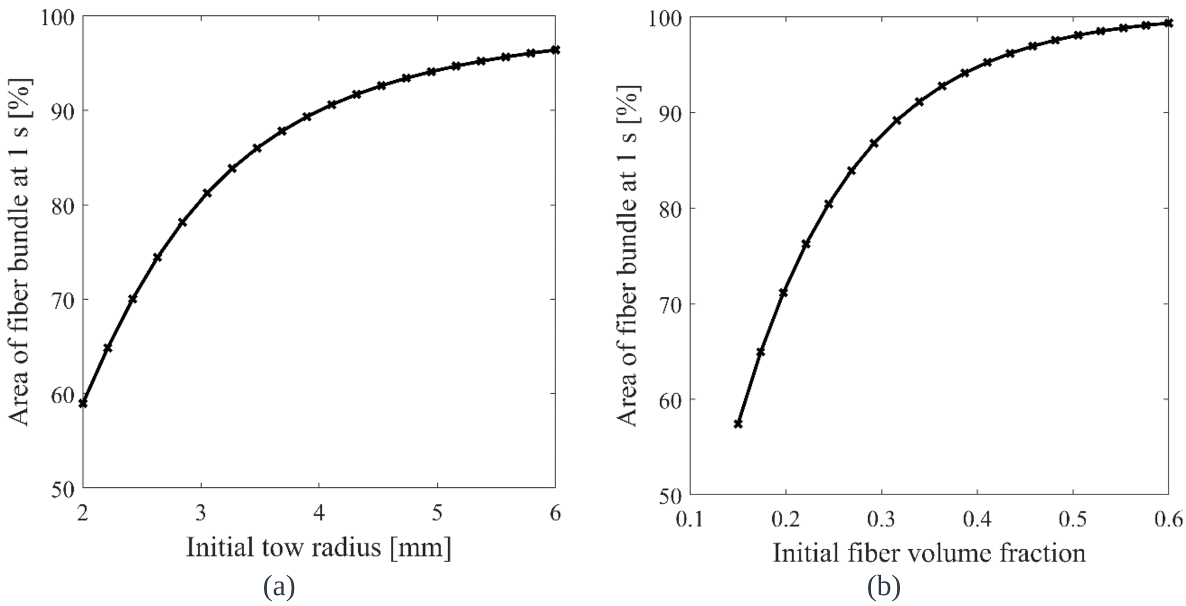

Figure 9: Cross-sectional area reduction after 1 second of braid pressure, shown for (a) various initial tow radii and (b) initial fiber volume fraction.

The previous results display little consolidation in tows with large radii due to insufficient pressures being applied by the braid. Figure 10 predicts what yarn tension is needed to decrease the fiber bundle area in size by 10%. If this consolidation threshold is desired, the tension settings on the individual bobbins can be adjusted to achieve the prescribed braid pressure.

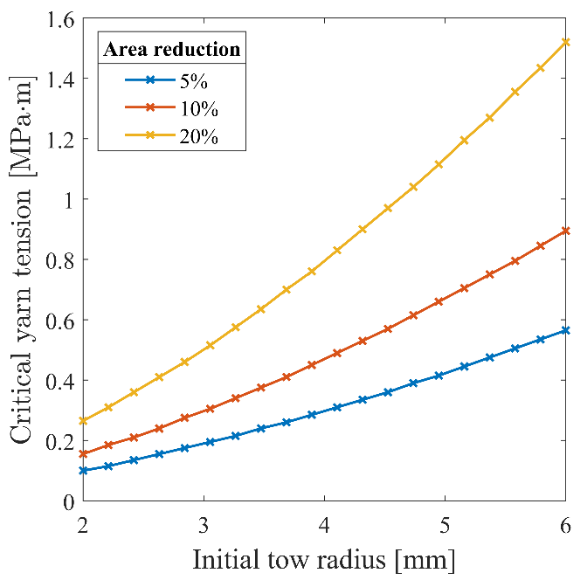

Figure 10: Critical yarn tension (F) needed for 5%, 10%, or 20% reduction of fiber bundle area.

4 CONCLUSIONS

Using the designated properties for the polypropylene and fiber system, the presented consolidation model can successfully simulate the influence that the circumferential pressure applied by the overbraid has on the radius and volume fraction of the fiber bundle. For a representative tow sample with an initial radius of 2.5 mm and initial volume fraction of 0.18, the sample consolidation was improved by ~20% when a circumferential pressure was applied by the overbraid with a yarn tension of 0.3 MPa·m. Micrographs of produced samples showed consolidation occurred in a time of roughly one second. This information was also used to extend the model to tows of various radii and fiber volume fraction to predict consolidation and performance.

It was found that higher fiber volume fractions and larger tows take longer time or larger pressures to consolidate. These results will be used to develop a robust processing window for this novel manufacturing line where line speed, temperature, and applied braid pressure and density can be manipulated. Additionally, by having a better understanding of how the volume fraction changes within the tow, more accurate predictions of mechanical properties can be made to improve the reliability of CAE, thus expanding the applications where M-TOW® and hybrid molding can be confidently implemented.

ACKNOWLEDGEMENTS

This material is based upon work supported by the U.S. Department of Energy's Office of Energy Efficiency and Renewable Energy (EERE) under the Vehicle Technologies Office Award Number DE-EE0009203. In addition to thanking Ford Motor Company and the Department of Energy for funding this work, the authors wish to thank EELCEE Ltd/QEE-Composites for the production and support of the M-TOW® line. The authors recognize Carson Work for his efforts in manufacturing, polishing, and imaging the M-TOW® samples. The authors also thank Joseph Anderson and Alex Reichanadter for their guidance in creating the consolidation model.

REFERENCES

[1] M. D. Wakeman, E. Eble, P. Beyeler, T. Herrmann, and J.-A. E. Månson, "Hybrid thermoplastic composite beam structures integrating UD tow, stamped fabric, and over-injection/compression moulding," in *Eccm-11*, Rhodes, Greece, 2004. [Online]. Available: http://www.escm.eu.org/docs/eccm/B090.pdf

[2] M. D. Wakeman, P. O. Hagstrand, F. Bonjour, P. E. Bourban, and J. A. E. Månson, "Robotic tow placement for local reinforcement of glass mat thermoplastics (GMTs)," *Compos Part A Appl Sci Manuf*, vol. 33, no. 9, pp. 1199–1208, 2002, doi: 10.1016/S1359-835X(02)00086-6.

[3] W. Krause, O. Geiger, and F. Henning, "Local continuous-fibre reinforcement," *Kunststoffe International*, vol. 96, no. 2, pp. 1–4, 2006.

[4] K. Arnaut, M. A. Dimassi, B. Romahn, U. Atilla, and A. S. Herrmann, "Analysis of open-hole-tension plates made of short fibre thermoplastic and reinforced with

continuous fibre tailored inserts," *Journal of Thermoplastic Composite Materials*, 2020, doi: 10.1177/0892705720963539.

[5] N. Minsch, M. Müller, T. Gereke, A. Nocke, and C. Cherif, "3D truss structures with coreless 3D filament winding technology," *J Compos Mater*, vol. 53, no. 15, pp. 2077–2089, 2019, doi: 10.1177/0021998318820583.

[6] F. Henning, L. Kärger, D. Dörr, F. J. Schirmaier, J. Seuffert, and A. Bernath, "Fast processing and continuous simulation of automotive structural composite components," *Compos Sci Technol*, vol. 171, no. December 2018, pp. 261–279, 2019, doi: 10.1016/j.compscitech.2018.12.007.

[7] M. Fiorotto and G. Lucchetta, "Experimental investigation of a new hybrid molding process to manufacture high-performance composites," *International Journal of Material Forming*, vol. 6, no. 1, pp. 179–185, 2013, doi: 10.1007/s12289-011-1066-3.

[8] J. Kang, J. Lee, J. Kim, T. Ahn, and D. Ko, "Using Hybrid Molding Method," 2021.

[9] J. D. Miller, P. Blanchard, J. Dahl, and J. E. Mansson, "Tow placement effects on fiber waviness and tensile performance of 3D-tow reinforced hybrid-molded composites," *Composites Part B*, vol. 256, no. January, p. 110625, 2023, doi: 10.1016/j.compositesb.2023.110625.

[10] N. Jansson, W. D. Wakeman, and J.-A. E. Mansson, "Optimization of hybrid thermoplastic composite structures using surrogate models and genetic algorithms," *Compos Struct*, vol. 80, pp. 21–31, 2007, doi: 10.1016/j.compstruct.2006.02.036.

[11] N. Jansson, P. O. Hagstrand, M. D. Wakeman, and J. A. E. Månson, "Finite element modelling and testing of an injection moulded generic tow reinforced structure," *Compos B Eng*, vol. 36, no. 6–7, pp. 487–495, 2005, doi: 10.1016/j.compositesb.2005.04.002.

[12] A. G. Gibson and J. Manson, "Impregnation technology for thermoplastic matrix composites," 1992.

[13] Z. Cai, T. Gutowski, and S. Allen, "Winding and Consolidation Analysis for Cylindrical Composite Structures," *J Compos Mater*, vol. 26, no. 9, pp. 1374–1399, 1992.

[14] A. E. SCHEIDEGGER, *The Physics of Flow Through Porous Media*, no. (THIRD EDITION: 1974). University of Toronto Press, 1974. doi: 10.1097/00010694-195812000-00015.

[15] A. Reichanadter and J. A. E. Mansson, "Extending the Gutowski model to kidney-bean and elliptically shaped fibers," *J Compos Mater*, vol. 56, no. 8, pp. 1313–1318, 2022, doi: 10.1177/00219983221075415.

[16] D. Merhi, V. Michaud, L. Kampfer, P. Vuilliomenet, and J.-A. E. Manson, "Transverse permeability of chopped fibre bundle beds," *Compos Part A Appl Sci Manuf*, vol. 38, pp. 739–746, 2007, doi: 10.1016/j.compositesa.2006.09.006.

[17] B. T. Astrom, R. B. Pipes, and S. G. Advani, "On Flow through Aligned Fiber Beds and Its Application to Composites Processing," *J Compos Mater*, vol. 26, no. 9, pp. 1351–1373, 1992.

[18] J. W. Seo and W. Il Lee, "A Model of the Resin Impregnation in Thermoplastic Composites," *J Compos Mater*, vol. 25, 1991.

[19] J. Lavorata and J.-A. E. Mansson, "Conductive overbraid of continuous fiber thermoplastic composite tows," *Composites Part B*, 2023, doi: https://doi.org/10.1016/j.compositesb.2023.110678.

[20] J. Lavorata and J.-A. E. Mansson, "Conductive Multifunctional Composite Preform (M-TOW)," 63/341,724, 2022

[21] Eelcee-Ltd., “Over-braided hybrid material manufacturing system,” South Korea Patent 0103194, 2017

[22] T. G. Gutowski, Z. Cai, S. Bauer, D. Boucher, J. Kingery, and S. Wineman, “Consolidation Experiments for Laminate Composites,” *J Compos Mater*, vol. 21, no. 7, pp. 650–669, 1987, doi: 10.1177/002199838702100705.